2.G

Nuclear Physics **A204** (1973) 497—515; © *North-Holland Publishing Co., Amsterdam*

THE REACTION ^{26}Mg(d, τ)^{25}Na AND THE STRUCTURE OF ^{25}Na

JOACHIM JÄNECKE

Cyclotron Laboratory, Department of Physics, University of Michigan, Ann Arbor, Michigan 48105 †

Received 26 October 1972

Abstract: The nuclear structure of the nucleus ^{25}Na has been studied with the (d, τ) proton pick-up reaction on ^{26}Mg at a bombarding energy of 29 MeV with an energy resolution of 25 to 30 keV FWHM. Excited states in ^{25}Na have been measured up to excitation energies of 8 MeV. The experimental angular distributions show good agreement with the predictions from the standard distorted-wave Born-approximation theory (code DWUCK; non-local and finite range). However, the agreement is improved considerably if the procedure of Kunz, Rost and Johnson is applied which accounts approximately for strong couplings to inelastic channels in the initial and final (strongly deformed) nuclei. The influence of this treatment on the evaluation of spectroscopic factors has been investigated and was found to be particularly pronounced for $l = 0$ transitions. The measured spectroscopic factors are compared to those from other experimental work and from shell-model and Nilsson-model calculations.

E NUCLEAR REACTIONS ^{26}Mg(d, ^{3}He), $E = 29$ MeV; measured $\sigma(\theta)$. ^{25}Na deduced levels, l, π, S. Enriched target.

1. Introduction

The energy levels of ^{25}Na constitute the $T = \frac{3}{2}$ states of the $A = 25$ system. Good spectroscopic data for these states have become available only recently [1]). In contrast, extensive information existed about the $T = \frac{1}{2}$ states in the $A = 25$ system, and its rotational structure is well established [2]). The $T = \frac{3}{2}$, $A = 25$ system is amenable to shell-model and Nilsson-model calculations. Wildenthal [3]) has performed shell-model calculations in a truncated $1d_{\frac{5}{2}}$-$2s_{\frac{1}{2}}$ space, and his calculated spectroscopic factors can be compared to the experimental results. In addition, Becker *et al.* [4]) have pointed out a strong resemblance between the level schemes for the low excited states in ^{19}O and ^{25}Na due to the fact that the low-excitation spectra result from the coupling to $T = \frac{3}{2}$ of of three nucleons outside the ^{16}O core, neutrons in ^{19}O, protons in ^{25}Na. Moreover, Krämer *et al.* [1]) have established a close correspondence between the spectra of ^{23}Na and ^{25}Na. This correspondence is easy to understand by invoking the Nilsson model. The same Nilsson orbits are responsible for the structure of the ground and many excited states, and the observed shift of the positive- and negative-parity states relative to each other is probably due to a different deformation. Unfortunately, detailed band-mixing calculations seem to exist [5]) only for ^{23}Na.

† Supported in part by the US Atomic Energy Commission.

The excitation energies of states in ^{25}Na up to $E_x \approx 5.8$ MeV are well known from measurements of the ^{26}Mg(t, α) and ^{23}Na(t, p) reactions at $E_t \approx 6$ MeV by Hinds *et al.* [6]). Additional states up to $E_x \approx 8$ MeV have been seen by Krämer *et al.* [1]) with the ^{26}Mg(d, τ) reaction at $E_d = 52$ MeV. Becker *et al.* [4]) observed γ-rays from states up to $E_x \approx 4$ MeV following the ^{26}Mg(t, α) and ^{23}Na(t, p) reactions. They made the first spin-parity assignments for several excited states on the basis of γ-ray angular-correlation and branching-ratio measurements. Information on angular-momentum transfers and spectroscopic factors has become available only recently. Dehnhard and DeLong [7]) and Maher *et al.* [8]) observed angular distributions which led to l-value assignments for the transitions to the four energetically lowest states in the ^{26}Mg(d, τ) reaction at $E_d = 20.0$ (34.4) MeV and 23 MeV, respectively. Detailed spectroscopic information from the (d, τ) reaction at $E_d = 52$ MeV up to $E_x \approx 8$ MeV was obtained recently by Krämer *et al.* [1]). Several multiplets were not resolved in this experiment such as the ground state doublet (0–90 keV) or the triplet near $E_x = 4$ MeV (3928–3952–3995 keV). Analogue states with $T = \frac{3}{2}$ in ^{25}Mg have been studied by Détraz and Richter [9]) by means of the reaction ^{26}Mg(τ, α). The spectroscopic information obtained for these transitions is relevant to ^{25}Na.

The nucleus ^{26}Mg is strongly deformed [10]), and another motivation for investigating the ^{26}Mg(d, τ) reaction was to study the influence of deformations on the angular distributions. The procedure of Kunz *et al.* [11]) has been used in the present work. These authors have shown that the effects of strong couplings to inelastic channels in the initial and final nucleus can be simulated approximately with a modified DWBA procedure. The procedure has already been applied earlier by Dehnhard and DeLong [ref. [7])] to their 20 MeV data, and the calculated distributions for the transitions to the states at 0, 90 and 1068 keV showed improvement. Krämer *et al.* [1]) have also used a modified DWBA analysis based on the phenomenological rule of Kaschl *et al.* [12]).

2. Experimental procedure

The experiment was performed with 29.0 MeV deuterons from the University of Michigan 83 inch cyclotron. The beam is analyzed and focused onto the target by two beam-preparation magnets. For some of the forward-angle measurements the second of these magnets was used as a bending (and focusing) magnet only by removing the beam-defining slits in the scattering chamber.

Targets with thicknesses of about 40 $\mu g \cdot cm^{-2}$ were prepared by vacuum deposition of isotopically enriched ^{26}Mg (99.7 %) onto thin carbon backings. The material was evaporated as metal either directly or after reduction in a tantalum crucible from the oxide. The thickness of the target was determined by neutron activation using the University of Michigan Ford Nuclear Reactor. The decay of the γ-lines following the β-decay of ^{27}Mg was measured in a Ge detector for several half-lives. A second value was deduced from the yield of deuterons elastically scattered from ^{26}Mg in the angular range 20°–35°. The value was obtained by comparing the experimental

differential cross section at the secondary peak near $\theta_{c.m.} = 32°$ with that predicted on the basis of the optical parameters used in the distorted-wave analysis. The results from the two methods agree reasonably well, and the estimated uncertainty in the overall normalization due to uncertainties in the target thickness and other factors is $\pm 20\,\%$.

All measurements were taken with the first of the three-stage magnetic spectrograph [13]). The angular range was from 6° to 45°, and the angular resolution was $\pm 2°$. The ^{3}He particles from the (d, τ) reaction on ^{26}Mg were detected in the focal plane by means of photographic emulsions or position-sensitive detectors. The emulsions were Ilford type K 0 of thickness 100 μm. Aluminum absorbers were placed in front of the plates to absorb the α-particles and to facilitate the selection of helion tracks from deuteron and proton tracks on account of their greater ionization density. A background of deuterons of the same magnetic rigidity originated from the beam-defining slits in the scattering chamber with subsequent elastic scattering in the target. This background was reduced by removing these slits and, for essentially all measurements below 15°, by simultaneously using up to five position-sensitive detectors in the focal plane instead of photographic plates. A monitor was used for all forward-angle measurements. The photographic plates were read by human scanners.

3. Distorted-wave analysis

3.1. SPECTROSCOPIC FACTORS

Spectroscopic factors C^2S have been obtained by comparing the experimental differential cross sections to the predictions from the distorted-wave theory. The calculations were performed with the computer code DWUCK [14]) using the local-energy approximation for non-local and finite-range effects. We have

$$\frac{\mathrm{d}\sigma}{\mathrm{d}\Omega}(\theta) = 29.5\, C^2 S_{lj} \frac{\sigma_{lj}(\theta)}{2j+1} . \tag{1}$$

Here, $(\mathrm{d}\sigma/\mathrm{d}\Omega)(\theta)$ are the experimental values in mb/sr, $\sigma_{lj}(\theta)$ are the reduced cross sections computed with DWUCK for pick-up from the orbital (l, j), S_{lj} is the conventional spectroscopic factor [15]), and C is a Clebsch-Gordan coefficient which ensures isospin conservation. For proton pick-up we have $C^2 = 2T_f/(2T_f+1)$. For our special reaction $C^2 = \frac{3}{4}$. The coefficient 29.5 has been evaluated by Bassel [16]) in the finite-range approximation. No summation over different l-values is required since the target has spin $J = 0$.

3.2. OPTICAL POTENTIALS

The general form of the optical potential has been employed. Parameter sets for the deuteron and helion potentials are listed in table 1. The deuteron parameters were obtained from the expressions given by Newman *et al.* [17]) for the Z- and A-dependent average set. The first set of the ^{3}He potential parameters is the energy-

TABLE 1

Optical-model parameter sets used in the distorted-wave analysis

Projectile	Set	V (MeV)	r_0 (fm)	a (fm)	W_0 (MeV)	W_D (MeV)	r'_0 (fm)	a' (fm)	$V_{s.o.}$ (MeV)	r_C (fm)	Ref.
d		93.78	1.054	0.814	0.00	10.85	1.360	0.729	6.74	1.300	[17]
τ	I	178.00	1.140	0.723	15.30	0.00	1.640	0.910	0.00	1.400	[18]
τ	II	143.40	1.140	0.723	23.80	0.00	1.600	0.810	0.00	1.400	[19]
τ	III	166.70	1.100	0.716	29.50	0.00	1.448	0.913	0.00	1.400	[19]
p (bound state)		adjusted	1.200	0.650					$\lambda_{s.o.} = 25$	1.250	

dependent set of Gibson *et al.* [18]) obtained for elastic scattering on ^{40}Ca for energies ranging from 22 to 64 MeV. The two other sets were used by Wildenthal and Newman[19]) in their analysis of the (d, τ) reaction on ^{27}Al. The parameters are related to the fixed geometry of Gibson, but the well depths were adjusted to fit several angular distributions of ^{3}He elastic scattering data on 1d-2s shell nuclei. The three ^{3}He parameter sets describe the experimental distribution for the (d, τ) ground state transition in ^{25}Na about equally well (see below).

3.3. BOUND-STATE WAVE FUNCTION

The bound-state wave function for the transferred proton was taken to be a single-particle wave function generated in a Woods-Saxon potential well. The depth was adjusted to give the correct binding energy of 5.494 MeV$-Q$(g.s.)$+E_x$. Standard geometrical parameters were used and are listed in table 1. Included in the binding potential is a spin-orbit coupling term of magnitude $\lambda_{s.o.} = 25$ times the Thomas term. Since this term has opposite sign for $j = l \pm \frac{1}{2}$, the effect on the wave function (for the same binding energy and assumed $j = l+\frac{1}{2}$ or $j = l-\frac{1}{2}$) leads to somewhat different spectroscopic factors while the shape of the angular distributions is affected only little.

3.4. CORRECTIONS FOR NON-LOCALITY AND FINITE RANGE

The necessity for applying corrections due to non-locality and finite-range effects in (d, τ) reactions has been pointed out by Hiebert *et al.* [20]). In the local energy approximation the corrections from both effects are approximately described by introducing radial correction factors which reduce the contributions to the reaction from the nuclear interior. The net effect of these corrections is to increase the predicted reaction cross sections and to decrease the spectroscopic factors. The shapes of the predicted angular distributions, however, appear not to be sensitive to these corrections.

In the present analysis the following non-locality range parameters were used: β(d) = 0.54, $\beta(\tau)$ = 0.30, β(p) = 0.00. The finite-range parameter R(d, τ) = 0.77 fm

was used. Note that the finite-range parameters used by Kunz [14]) in his code DWUCK and that of Bassel [16]) differ by a factor of two.

3.5. CORRECTIONS FOR STRONG COUPLINGS TO INELASTIC CHANNELS

The effects of strong couplings to inelastic channels in the initial and final nuclei can be important in particle-transfer reactions, particularly on deformed nuclei. Kunz *et al.* [11]) introduced an approximate procedure to account for these effects by adding a term $\kappa V_\lambda(r)$ to the spherical potential $V(r)$ used in the coupled-channels calculations. The procedure makes use of the adiabatic approximation, a smoothness approximation, and a limitation to a first-order term in the coupling. For deformed nuclei the approximation can be represented by a change in the radii of the optical-model potentials which describe the distorted waves of the incoming and outgoing particles. The radii have to be increased by the factor $(1+\kappa\beta)$ where β is the deformation parameter and κ depends on the Nilsson coefficients. An explicit expression for κ is given by Kunz *et al.* [11]) for cases where the target nucleus is doubly even and the coupling term is due to the quadrupole deformation. Their table II lists numerical values for κ for levels based on Nilsson orbits 7 and 6 (not 11; for notation see table 3) which are also of interest in the ^{26}Mg(d, τ) ^{25}Na reaction. It appears that band-mixing calculations for κ have not yet been performed.

3.6. THE RULE OF KASCHL *ET AL.*

Kaschl *et al.* [12]) in their analysis of (d, τ) reactions at $E_d = 52$ MeV on a variety of 1d-2s shell nuclei [see also ref. [1]) and references quoted therein] compared the observed variations of the phases of the forward maxima and minima with the predictions from the distorted-wave theory. They observed discrepancies and found empirically that better agreement can be obtained by modifying the real radius parameters of both optical potential wells and that of the bound-state potential well without changing any of the other potential parameters. As a phenomenological rule they introduced shell-dependent real potential radii according to $r_0 16^{\frac{1}{3}}$ for pick-up from the 1p shell, $r_0 28^{\frac{1}{3}}$ for the $1d_{\frac{3}{2}}$ shell, $r_0 32^{\frac{1}{3}}$ for the $2s_{\frac{1}{2}}$ shell, and $r_0 40^{\frac{1}{3}}$ for the $1d_{\frac{5}{2}}$ shell rather than the ordinarily required radii $r_0 A^{\frac{1}{3}}$.

4. Experimental results

Fig. 1 shows a ^{3}He spectrum obtained at $\theta_{lab} = 15°$. The spectrum is a composite of several overlapping exposures with different magnet settings. It covers states in ^{25}Na up to excitation energies of 8 MeV. The resolution of 27 keV is due to target thickness and other factors. Lines from the carbon backing and from oxygen contaminations interfere with the lines of interest at a few select angles. The spectrum is dominated by a strong $l = 2$ pick-up transition to the ground state. The state at $E_x = 5190$ keV is the energetically highest state which carries sizable spectroscopic strength.

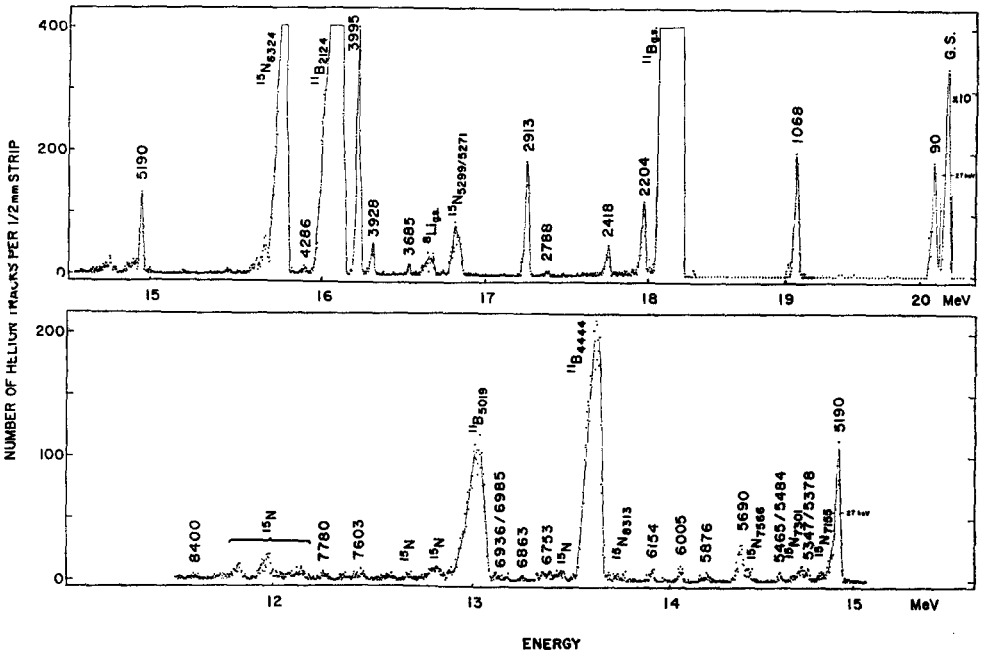

Fig. 1. Spectrum of ^{3}He particles from the reaction ^{26}Mg(d, τ)^{25}Na obtained with 29 MeV deuterons and photographic plates in the focal plane of the first analyzer magnet at $\theta_{lab} = 15°$. The spectrum is a composite of several overlapping exposures.

The experimental angular distributions for the various transitions are shown in figs. 2–5. They are labeled by the excitation energies. The DWBA predictions shown with the data will be discussed later. Figs. 2–4 show the distributions which are characteristic for $l = 2$, $l = 0$ and $l = 1$, respectively, while fig. 5 shows all transitions which are weak and/or exhibit angular distributions characteristic for high-angular-momentum transfers. All transitions to known states with excitation energies up to 6005 keV are included in the figures except for the transitions to the states at 3456 keV and 3952 keV. These transitions are weaker than that to the state at 3685 keV, and they cannot be seen in the presence of background or stronger neighboring lines. Also not shown are the weak transitions to the states above 6005 keV which have been measured at three angles only. These include transitions to eight states which have not been observed before. They are listed in table 3.

5. Discussion

5.1. OPTICAL PARAMETERS AND CORRECTIONS FOR NON-LOCALITY AND FINITE RANGE

Fig. 6 shows the comparison between the measured angular distribution for the transition to the ground state and several predictions from the distorted-wave theory. The upper curves are based on the zero-range approximation (L/ZR). The lower

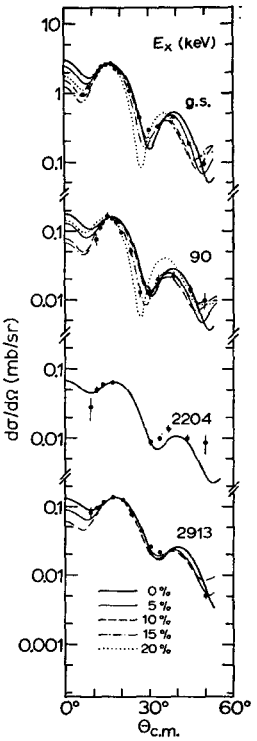

Fig. 2. Measured angular distributions with $l = 2$ characteristics. The heavy lines represent the predictions from the distorted-wave theory (non-local and finite range). The thin continuous, dashed, dash-dotted and dotted lines

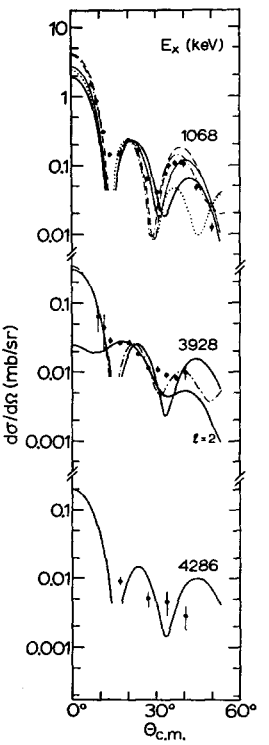

Fig. 3. Measured and calculated angular distributions with $l = 0$ characteristics. The distribution for the state at 3928 keV includes a calculated curve with $l = 2$ characteristics.

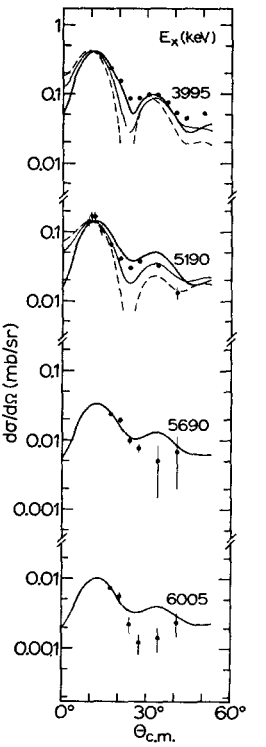

Fig. 4. Measured and calculated angular distributions with $l = 1$ characteristics.

are the result of the modified theory [11]) which includes corrections for couplings to inelastic channels. The percentages assigned to the curves represent the relative increases in the respective optical potential radii. The curves are labeled by the excitation energies taken from ref. [21]). (All cross sections of this and the other figures have to be multiplied by the factor 0.9.)

curves are based on the local-energy approximation for the corrections due to non-locality and finite range (NL/FR) with the parameters of sect. 3. The three respective curves were obtained by using the optical parameter sets of table 1. Parameter set I gives best agreement for L/ZR while there is a preference for set II for NL/FR. The behavior below $\theta_{c.m} = 12°$ is not reproduced by any of the calculated curves. Also, the experimental maximum near 16° appears somewhat sharper than the calculated curves.

The ^{3}He parameter set I and NL/FR were chosen for all subsequent comparisons. The use of sets II or III would lead to slightly reduced spectroscopic factors. The use

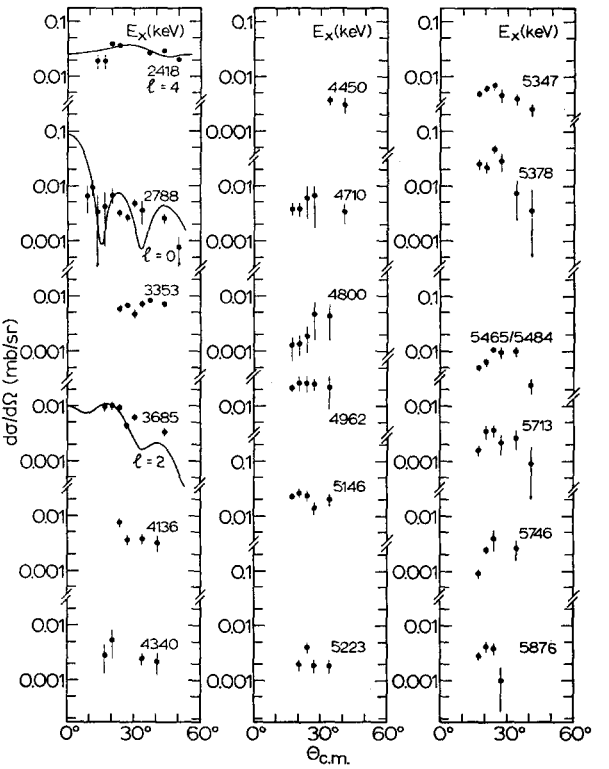

Fig. 5. Measured (and calculated) angular distributions with no particular angular characteristics.

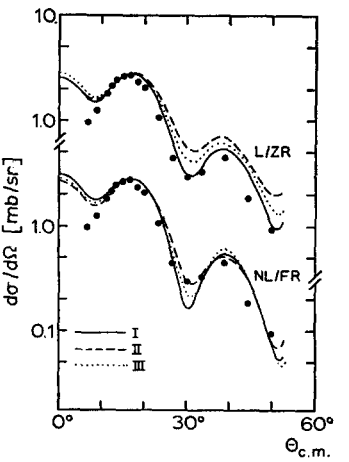

Fig. 6. Measured angular distribution for the transition to the ground state and comparison to the distorted-wave predictions with $l = 2$ using the three ^{3}He parameter sets of table 1 and the local/zero-range and non-local/finite-range approximations, respectively.

of L/ZR would lead to increased spectroscopic factors in agreement with the expectation expressed earlier. The increase is 22 % for the $l = 2$ ground state transition and is 51 % for the $l = 0$ transition to the state at 1068 keV. Thus, the use of L/ZR would lead to a general increase with a pronounced enhancement of the $l = 0$ spectroscopic strength. The curves displayed in figs. 2–5 as heavy lines are based on the above assumptions. The other curves will be explained below. Most assignments of l-values are unambiguous with only a few exceptions.

5.2. THE $l = 2$ TRANSITIONS

Fig. 2 shows the transitions which display $l = 2$ characteristics. The ground state in ^{25}Na is well known [21]) to have $J^\pi = \frac{5}{2}^+$. Angular distributions for the (d, τ) reaction with $l = 2$ have been observed before [1, 7, 8]). The state at 90 keV has been assigned $J = \frac{3}{2}$ or $\frac{5}{2}$ from γ-ray correlation and branching ratio measurements [4]), and an angular distribution with $l = 2$ has been observed before [7]). Even though a direct determination of the assignment $J = \frac{3}{2}$ appears not to exist, it seems to be favored by theoretical arguments [see ref. [4])]. The states at 2204 keV and 2913 keV have been assigned $J = \frac{3}{2}$ and $J = \frac{3}{2}$ or $\frac{5}{2}$ from γ-ray measurements [4]). Angular distributions with $l = 2$ characteristics for these two states have been observed before [1]). The assignment $J = \frac{5}{2}$ for the latter state is more likely on theoretical grounds as it is probably the second $\frac{5}{2}^+$ state of the two rotational bands (see below) based on $K^\pi = \frac{3}{2}^+$ (90 keV) and $K^\pi = \frac{1}{2}^+$ (1068 keV). Another $\frac{5}{2}^+$ state is also required by shell-model calculations [3]).

5.3. THE $l = 0$ TRANSITIONS

Fig. 3 shows the transitions which display $l = 0$ characteristics. The state at 1068 keV has been assigned $J^\pi = \frac{1}{2}^+$ from γ-ray measurements [4]), and angular distributions with $l = 0$ have been observed before [1, 7, 8]). The state at 3928 keV had no spin assignment. The finite resolution in the experiment of Krämer *et al.* [1]) precluded its separation from the strong $l = 1$ transition to the state at 3995 keV. The probable assignment of $l = 0$ for this relatively weak transition from the present experiment is based on the comparison of the measured angular distribution and of the measured ratio for the states 3928 keV/3995 keV with distorted-wave predictions. A possible assignment of $l = 2$ cannot be completely excluded, though. The state at 4286 keV has been assigned $J^\pi = \frac{1}{2}^+$ from an $l = 0$ angular distribution [1]). This assignment has been adopted here because the presence of lines from carbon and oxygen did not permit the measurement of a more complete angular distribution.

5.4. THE $l = 1$ TRANSITIONS

Fig. 4 shows the transitions which display $l = 1$ characteristics. The state at 3995 keV has been assigned $J^\pi = \frac{1}{2}^-$ on the basis of an $l = 1$ angular distribution [1]), and from the fact that it is the energetically lowest state resulting from pick-up from the 1p shell. The state at 5190 keV has been assigned $J^\pi = (\frac{1}{2}^-, \frac{3}{2}^-)$ on the basis of an $l = 1$ angular distribution [1]). Additional transitions with $l = 1$ angular characteristics

have been observed [1]) before for transitions to states at 5690, 6005, 6549, 6753, 7603 and 8052 keV. Angular distributions compatible with $l = 1$ are shown in fig. 4 for the first two of these transitions. No angular distributions were taken for the others.

5.5. OTHER TRANSITIONS

Fig. 5 shows the weak or unspecific angular distributions. The differential cross sections range from about 1 to 20 μb/sr. Many of the transitions could just barely be detected.

The state at 2418 keV has been given a probable assignment $J > \frac{5}{2}$ from γ-ray correlation and branching-ratio measurements [4]). A flat angular distribution has been observed in the (d, τ) reaction, and the comparison with a corresponding ^{24}Mg(d, τ) ^{23}Na transition suggests $J^\pi = \frac{7}{2}^+$ for this state [1]). The assignment is confirmed by the present data which are shown in fig. 5 together with the distorted-wave predictions for $l = 4$. The state at 2788 keV has been reported as $(\frac{1}{2}^+)$ from a (d, τ) angular distribution [1]). This assignment is not confirmed by the present experiment. Data points for this weak but well separated transition have been measured to small forward angles, and the comparison with the distorted-wave predictions for $l = 0$ are shown in fig. 5. (If the assignment $l = 0$ were adopted, the spectroscopic factor would be $C^2S \approx 0.02$; not shown on table 3.) The assignment $J \geqq \frac{3}{2}$ has been given for the state at 3353 keV based on γ-ray measurements [4]). No assignment is possible from the present experiment, but it excludes a direct reaction with $l \leqq 2$. The state at 3685 keV has been reported as $(\frac{5}{2}^+)$ from a (d, τ) angular distribution [1]). The present data shown on fig. 5 with the predictions for $l = 2$ do not support this assignment but cannot exclude it. (If the assignment $l = 2$ were adopted, the spectroscopic factor would be $C^2 \approx S$ 0.03; not shown on table 3.) In addition to the transition to the state at 2418 keV, three more transitions (to the states at 4962 keV, 5146 keV, and 5378 keV) exhibit cross sections which are at least a factor four stronger than the remaining transitions. Weak direct transitions could possibly be considered for these states.

5.6. CORRECTIONS FOR STRONG COUPLINGS TO INELASTIC CHANNELS

It was mentioned earlier that the agreement between the experimental and calculated distributions for the $l = 2$ ground state transition is not very good at the forward angles (see figs. 6 and 2). The situation for the weak $l = 2$ transition to the state at 90 keV is very similar. For the $l = 0$ transition to the state at 1068 keV the agreement is even worse at the forward angles, and the secondary maxima, in particular the one near $\theta_{c.m.} = 39°$, occur at angles considerably smaller than predicted (see fig. 3). Since ^{26}Mg is a strongly deformed nucleus [10]), it was decided to apply the procedure of Kunz *et al.* [11]) to correct for the effects of strong couplings to inelastic channels. The respective thin lines in figs. 2–4 for the above and several other states (solid, dashed, dash-dotted, dotted) show the results for optical potential radii increases of 5 %, 10 %, 15 %, and 20 %, respectively. As one can see from the figures,

TABLE 2

Comparison between the experimental and calculated coefficients $\kappa\beta$ (%)

E_x (keV)	J	Experimental	Calculated	
			Nilsson orbit 7	Nilsson orbit 6
0	$\frac{5}{2}^+$	8±3	3	11
90	$\frac{3}{2}^+$	14±3	12	25
1068	$\frac{1}{2}^+$	13±5		19
2204	$\frac{3}{2}^+$	6±5		
2913	$\frac{5}{2}^+$	3±3		
3928	$\frac{1}{2}^+$	15±5		
3995	$\frac{1}{2}^-$	< 3		
5190	$\frac{3}{2}^-$	5±4		
5690	$\frac{3}{2}^-$	≈ 0		
6005	$\frac{3}{2}^-$	≈ 0		

The coefficients account for couplings to inelastic channels [11]).

the procedure leads to considerably better agreement between the shapes of the experimental and calculated distributions. Best agreement is obtained for the increases shown in table 2. Dehnhard and DeLong [7]) applied the same procedure to their 20 MeV data and reported percentages of 10–20 for the three energetically lowest transitions in agreement with the present results. Kunz *et al.* [11]) have reported numerical values for the coefficient κ for Nilsson orbits 7, i.e., $[211]\frac{3}{2}^+$, and orbit 6, i.e., $[220]\frac{1}{2}^+$, and the values $\kappa\beta$ with $\beta = 0.28$ are also shown in the table for comparison.

The $\frac{5}{2}^+$ ground state has presumably strong contributions from Nilsson orbit 7 (see the end of subsect. 5.8 for details about the Nilsson wave functions and the correspondence between ^{23}Na and ^{25}Na). The calculated value of 3 % is smaller than the observed one. However, the wave function of Dubois [5]) for the corresponding state at 390 keV in ^{23}Na suggests considerable amounts of band mixing with Nilsson orbits 6, 9 and even 5 which may well account for the observed value.

The wave function [5]) for the $\frac{3}{2}^+$ state at 90 keV in ^{25}Na which corresponds to the ground state of ^{23}Na is almost pure and based on Nilsson orbit 7. Indeed, the calculated value of 12 % agrees very well with the experimental value of (14±3) %.

The $\frac{1}{2}^+$ state at 1068 keV in ^{25}Na presumably corresponds to the energetically lowest $\frac{1}{2}^+$ state in ^{23}Na at 2391 keV. As discussed in subsect. 5.8, this state is probably based on Nilsson orbit 6, and the agreement between the experimental and calculated values is again quite good. However, there appear to exist discrepancies for the three observed $\frac{1}{2}^+$ states with respect to the wave functions of Dubois [5]) and the measured spectroscopic factors. Because of this observation and since band-mixing calculations for κ seem not to exist, no further attempts have been made for a comparison between experimental and calculated values of $\kappa\beta$.

To facilitate the comparison between the shapes of the experimental and calculated angular distributions, the curves have generally been normalized at the first maximum.

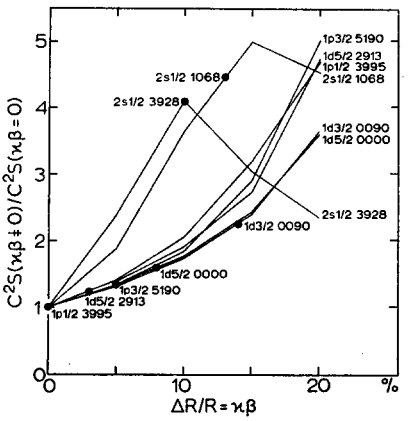

Fig. 7. Plot for several transitions of the multiplication factors for the spectroscopic factors C^2S to be used in the procedure of Kunz *et al.* [11]). The abscissa is $\Delta R/R = \kappa\beta$. The points are based on the best estimate for $\Delta R/R$. They are labeled by the spectroscopic assignment and the excitation energy in keV.

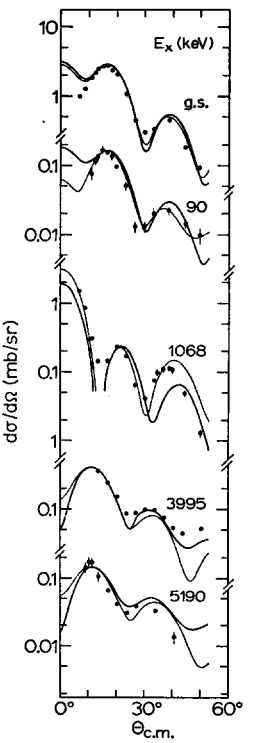

Fig. 8. Measured angular distributions for the transitions to the states at 0 keV ($1d_{\frac{5}{2}}$), 90 keV ($1d_{\frac{3}{2}}$), 1068 keV ($2s_{\frac{1}{2}}$), 3995 keV ($1p_{\frac{1}{2}}$) and 5190 ($1p_{\frac{3}{2}}$). The heavy lines represent the predictions from the unmodified distorted-wave theory (non-local and finite range). The thin lines are obtained by applying the phenomenological rule of Kaschl *et al.* [12]).

A change in the optical potential radii by the factor $1+\kappa\beta$, however, will also lead to a change in the spectroscopic factors extracted from the data. This change is considerable, particularly for $l = 0$ transitions, as can be seen from fig. 7. Here, the ratio of the spectroscopic factors obtained with and without the radius correction is plotted as a function of $\Delta R/R = \kappa\beta$. The heavy points are based on the best estimate for $\kappa\beta$. For the $l = 2$ transitions to the states at 0 keV, 90 keV, and 2913 keV, the spectroscopic factors are increased by factors of 1.6, 2.3, and 1.2, respectively. For the $l = 1$ transitions to the states at 3995 keV and 5190 keV, the increases are by factors of 1.0 and 1.3, respectively. For the $l = 0$ transitions to the states at 1068 keV and 3928 keV, finally, the increases are by factors of 4.5 and 4.1, respectively. The latter result confirms the enormous sensitivity of $l = 0$ spectroscopic factors to the details of the calculation. The use of L/ZR would enhance the $l = 0$ strength even further by about 30 %.

5.7. THE RULE OF KASCHL *ET AL.*

The phenomenological rule of Kaschl *et al.* [12]) recommends the use of shell-dependent real potential radii. Fig. 8 shows for several transitions the change of the calculated distributions which results from the application of the above rule. The agreement with the measured angular distributions is indeed improved for the transitions to the states at 90 keV ($l = 2$) and 1069 keV ($l = 0$). In contrast, the agreement at the forward angles for the strong ground state transition ($l = 2$) is not improved at all. Only slight changes in the calculated distributions are observed for the transitions to the states at 3995 keV ($l = 1$) and 5190 keV ($l = 1$). Because of the above inconclusive results, no further attempts have been made to apply this empirical rule.

5.8. SPECTROSCOPIC FACTORS C^2S

The spectroscopic factors C^2S from the present work are listed in columns 3, 4 and 5 of table 3. They were obtained in several ways. The values of column 3 are those of the non-modified distorted-wave theory in the NL/FR approximation. The total spectroscopic strength for transitions to states with $J^\pi = \frac{5}{2}^+$, $\frac{3}{2}^+$ and $\frac{1}{2}^+$ is $\sum C^2S(\text{1d-2s}) \approx 3.5$. This value is only slightly below the simple shell-model estimate of 4.0. If the procedure of Kunz *et al.* [11]) is employed to account for couplings to inelastic channels, the values in column (4) are obtained. The multiplication factors of fig. 7, based on the experimental values of $\Delta R/R = \kappa\beta$, have been used. Estimated factors were used for a few weak transitions. The total spectroscopic strength becomes $\sum C^2S(\text{1d-2s}) \approx 6.1$ which represents a considerable overestimate of the simple shell-model expectation. It should be noted that the use of L/ZR would lead to an additional increase of the absolute spectroscopic factors by about 20 to 50 %.

The overestimate of the added 1d-2s shell spectroscopic strength may be due to the fact that in the procedure of Kunz *et al.* [11]) the changes in the bound-state wave function are not included. However, Rost [22]) has shown that bound-state wave functions generated in a deformed potential well are generally reduced in the nuclear

TABLE 3

Summary of the experimental and theoretical spectroscopic factors C^2S for the proton pick-up reaction $^{26}Mg(d, \tau)^{25}Na$

(1)	(2)	(3)	(4)	(5)	(6)	(7)	(8)	(9)	(10)
Level [a]		C^2S[(d, τ), 29 MeV] [b]			C^2S(d, τ)[c]	$C^2S(\tau, \alpha), T_>$[d]	Level		C^2S [e]
E_x (keV)	J^π	NL/FR	NL/FR ($\beta\kappa \neq 0$)	NL/FR ($\beta\kappa \neq 0$) normalized	L/ZR	L/ZR normalized	E_x (keV)	J^π	shell model
0	$\frac{5}{2}^+$	2.56	4.11	2.61	3.02	2.70	0	$\frac{5}{2}^+$	2.72
90	$\frac{3}{2}^+$	0.22	0.51	0.33		0.32	60	$\frac{3}{2}^+$	0
1068	$\frac{1}{2}^+$	0.13	0.55	0.35	0.33	0.28	760	$\frac{1}{2}^+$	0.55
2204	$\frac{3}{2}^+$	0.15	0.23	0.15	0.09		3100	$\frac{3}{2}^+$	0
2418	$(\frac{3}{2}^+)$	(0.49)	(0.49)	(0.31)			2140	$\frac{7}{2}^+$	0
2788					[f]				
2913	$(\frac{5}{2}, \frac{3}{2})^+$	0.30	0.37	0.24	0.32	0.35	2730	$\frac{5}{2}^+$	0.50
3353	$\geqq \frac{3}{2}$								
3685					[f]				
3928	$(\frac{1}{2}^+)$	(0.06)	(0.27)	(0.17)			4290	$\frac{1}{2}^+$	0.00
3995	$(\frac{1}{2}, \frac{3}{2})^-$	1.05	1.05	0.67	2.41	1.48			
4286	$\frac{1}{2}^+$	0.05	0.10	0.06	≈ 0.10		6710	$\frac{1}{2}^+$	0.01
5190	$(\frac{3}{2}, \frac{1}{2})^-$	0.56	0.75	0.47	≈ 0.85	0.55			
5690	$(\frac{3}{2}, \frac{1}{2})^-$	0.16	0.16	0.10	0.20		2310	$\frac{9}{2}^+$	0
6005	$(\frac{3}{2}, \frac{1}{2})^-$	0.06	0.06	0.04	0.10		3620	$\frac{7}{2}^+$	0
6549	$(\frac{3}{2}, \frac{1}{2})^-$				0.22		4470	$\frac{3}{2}^+$	0
6753	$(\frac{3}{2}, \frac{1}{2})^-$				< 0.12		4620	$\frac{9}{2}^+$	0
7603	$(\frac{3}{2}, \frac{1}{2})^-$				0.30		4660	$\frac{5}{2}^+$	0.01
8052	$(\frac{3}{2}, \frac{1}{2})^-$				< 0.18		5040	$\frac{5}{2}^+$	0.02

[a]) Excitation energies from ref. [21]) and for $E_x > 6000$ keV from ref. [1]). New levels have been found at $E_x = 5876 \pm 12$, 6079 ± 15, 6154 ± 15, 6863 ± 20, 6936 ± 20, 6985 ± 20, 7780 ± 25 and 8400 ± 25 keV. For additional levels of which the angular distributions have no particular angular characteristics, see fig. 5.

[b]) Present work.

[c]) Ref. [1]); $E_d = 52$ MeV.

[d]) Transitions to $T = \frac{3}{2}$ analogue states in ^{25}Mg; ref. [9]); $E_\tau = 14.5$ MeV.

[e]) Ref. [3]).

[f]) The assignments $(\frac{1}{2}^+)$ and $(\frac{3}{2}^+)$ with spectroscopic factors of ≈ 0.06 and ≈ 0.08, respectively, are not listed here.

interior and enhanced in the exterior. The use of bound-state wave functions from a deformed well instead of a spherical well should therefore decrease the spectroscopic factors similarly to the decrease observed with the use of NL/FR instead of L/ZR. Indeed, Broad [23]) has carried out preliminary calculations for the energetically lowest states in ^{25}Na based on the wave functions by Dubois [5]) for the corresponding states in ^{23}Na. He finds considerable reduction factors for C^2S, namely about 0.53 for the $\frac{5}{2}^+$ ground state, about 0.95 for the $\frac{3}{2}^+$ state at 90 keV, and about 0.90 (or 0.40) for the $\frac{1}{2}^+$ state at 1068 keV. The latter two values are obtained depending on whether this $\frac{1}{2}^+$ state is assumed to be based on Nilsson orbit 6 or 9, respectively. When these factors are applied, the total spectroscopic strength for the 1d-2s shell is again reduced

to a value slightly below the expected value of 4.0. This result is very reassuring and points to the internal consistency of the whole approach. However, it also shows that spectroscopic factors extracted for the weaker transitions in reactions on deformed nuclei may well be uncertain by a factor of 2.

Because of the limited knowledge about the wave functions and the preliminary nature of the bound-state wave function calculations, the above approach has not been pursued further. Instead a general reduction factor of about 0.63 was applied to all values of column 4. Column 5 shows the result which amounts to a renormalization of the total spectroscopic strength to $\sum C^2S(1d\text{-}2s) = 3.9$. A value slightly below 4.0 was chosen to account for some unobserved spectroscopic strength to higher excited states.

A comparison between the spectroscopic factors from the present experiment (columns 3 and 5) and those from other experimental work (columns 6 and 7) shows good agreement, particularly for the 1d-2s shell states. The $l = 0$ strength for the state at 1068 keV appears to be too weak in the unmodified distorted-wave analysis, but the corrected value of column 5 agrees very well. The observed 1p strength is weaker than the one observed in the other experiments. This is particularly the case for the $l = 1$ transition to the $(\frac{1}{2}, \frac{3}{2})^-$ state at 3995 keV in the corrected procedure.

Wildenthal [3]) has carried out a shell-model calculation for ^{25}Na based on a truncated $1d_{\frac{5}{2}}$-$2s_{\frac{1}{2}}$ space. Because of the limited shell-model space, spectroscopic strength is predicted only for levels with $J^\pi = \frac{5}{2}^+$ and $\frac{1}{2}^+$. Except for this limitation, the agreement between the experimental and calculated level schemes and the spectroscopic factors is quite good. Several calculated levels for which the corresponding experimental levels have not been established are included in the list.

The observed $1d_{\frac{5}{2}}$ strength of $C^2S = 2.56/2.61$ for the strong transition to the $\frac{5}{2}^+$ ground state agrees well with the predicted value of $C^2S = 2.72$. Additional $1d_{\frac{5}{2}}$ strength is observed for the transition to the state at 2913 keV. The calculation seems to slightly overestimate this component. A possible candidate for one of the two predicted $\frac{5}{2}^+$ states at higher energy (4660 keV and 5040 keV) is the state at 5378 keV. A substantial amount of $1d_{\frac{3}{2}}$ strength has been observed for the transitions to the $\frac{3}{2}^+$ states at 90 keV and 2204 keV. No strength is predicted for these states, of course. The observed $2s_{\frac{1}{2}}$ strength of $C^2S = 0.13/0.35$ for the transition to the $\frac{1}{2}^+$ state at 1068 keV is weaker than the predicted value of $C^2S = 0.55$ but still the strongest of the three observed $l = 0$ transitions. Two higher $\frac{1}{2}^+$ excited states are populated weakly while the predicted strength is practically zero. Several states with $J^\pi = \frac{7}{2}^+$ and $\frac{9}{2}^+$ are predicted with no spectroscopic strength, but only one experimental state can be related to it with confidence. The observed state at 2418 keV has probably $\frac{7}{2}^+$ and corresponds to the state predicted at 2140 keV. The observed strength of $C^2S = 0.49/0.31$ appears too big for a $1g_{\frac{7}{2}}$ admixture in the ground state wave function of ^{26}Mg. Therefore, a two-step process cannot be excluded. A similar situation has been observed at the same bombarding energy for the transition to the $\frac{7}{2}^+$ state at 7570 keV in the ^{16}O(d, τ)^{15}N reaction [24]). The observed state at 2788 keV

is a likely candidate for the predicted $\frac{9}{2}^+$ state at 2310 keV. It is worth adding that the results of shell-model calculations for ^{19}O, for example those of Federman [24]), strongly resemble the results for ^{25}Na of Wildenthal [3]). The reason is that in both nuclei the low-excitation spectra result from the coupling of $T = \frac{3}{2}$ of three nucleons. The calculations for ^{19}O also predict a $\frac{9}{2}^+$ state at about the same excitation energy, and such a state has indeed been observed [26]) in ^{19}O at 2775 keV.

The energetically lowest state with negative parity at 3995 keV must be based on a $1p_{\frac{1}{2}}$ hole. The observed strength of $C^2S = 1.05/0.67$ exhausts part of the simple shell-model estimate of 2.0. The state at 5190 keV with $C^2S = 0.56/0.47$ is probably based on a $1p_{\frac{3}{2}}$ hole. Most of the additional states with negative parity at 5690 keV, 6005 keV and higher probably have $J^\pi = \frac{3}{2}^-$. If all observed transitions to states above 6005 keV were given an $l = 1$ assignment, their spectroscopic strength would add up to a value of about 1.1. Only a fraction of the expected $1p_{\frac{1}{2}}$ and $1p_{\frac{3}{2}}$ strength has been observed in the present experiment. The observed centroid energies for the 1p shell proton holes are $\gtrapprox$ 4000 keV ($1p_{\frac{1}{2}}$), > 5280 keV ($1p_{\frac{3}{2}}$) and > 4640 keV (1p).

Spectroscopic factors can also be calculated on the basis of the Nilsson model. Unfortunately, band-mixing calculations for ^{25}Na seem not to exist. On the other hand, detailed band-mixing calculations have been performed for ^{23}Na by Dubois [5]) to describe his data on the ^{22}Ne(τ, d)^{23}Na stripping reaction. Some of his conclusions can be applied to ^{25}Na because the level schemes of the two nuclei show a close correspondence [1]). The energetically lowest band is based on Nilsson orbit 7 characterized by $[211]\frac{3}{2}^+$. In ^{23}Na the $\frac{3}{2}^+$ band head is the ground state. The $\frac{5}{2}^+$ member of this band is energetically depressed due to strong mixing with other $\frac{5}{2}^+$ state and lies at 439 keV. In ^{25}Na, however, the $\frac{5}{2}^+$ state is apparently depressed even further and becomes the ground state. The $\frac{3}{2}^+$ band head lies at 90 keV. The $\frac{1}{2}^+$ states at 2391 keV in ^{23}Na and 1068 keV in ^{25}Na are the band heads of the next higher band. According to Dubois [5]) the band is based on orbit 9 with $[211]\frac{1}{2}^+$. However, the arguments presented below seem to make orbit 6 with $[220]\frac{1}{2}^+$ more likely. Table 4 lists the Nilsson orbits in their energetic sequence expected for large positive deformations.

To facilitate the discussion presented below, idealized spectroscopic factors for ^{26}Mg(d, τ)^{25}Na from the Nilsson model are shown in table 4. The values are obtained by using the tables of Chi [27]) with $\delta = 0.25$. It was assumed that there exists no band mixing and that the orbits in ^{26}Mg are completely filled up to and including orbit 7 and are empty beyond.

The $\frac{5}{2}^+$ ground state of ^{25}Na presumably corresponds to the state at 439 keV in ^{23}Na which has a strong calculated component [23]) from orbit 7 with additional contributions from orbits 6, 9 and even 5. The strong calculated spectroscopic factor of $C^2S = 1.90$ for pick-up from orbit 7 without band mixing still underestimates the observed strength. Preliminary band mixing calculations by Dehnhard [7]) indicate that band mixing indeed leads to an enhancement of the $1d_{\frac{5}{2}}$ strength for the ground state.

TABLE 4
Spectroscopic factors C^2S for the proton pick-up reaction ^{26}Mg(d, τ)^{25}Na assuming Nilsson wave functions [27]) with $\delta = 0.25$

Nilsson orbit	J	C^2S
3 $[110]\frac{1}{2}^-$	$\frac{1}{2}^-$	0.29
	$\frac{3}{2}^-$	1.71
2 $[101]\frac{3}{2}^-$	$\frac{3}{2}^-$	2.00
4 $[101]\frac{1}{2}^-$	$\frac{1}{2}^-$	1.71
	$\frac{3}{2}^-$	0.29
6 $[220]\frac{1}{2}^+$	$\frac{1}{2}^+$	0.53
	$\frac{3}{2}^+$	0.15
	$\frac{5}{2}^+$	1.32
7 $[211]\frac{3}{2}^+$	$\frac{3}{2}^+$	0.11
	$\frac{5}{2}^+$	1.90
9 $[211]\frac{1}{2}^+$	$\frac{1}{2}^+$	0.00 [0.40]
	$\frac{3}{2}^+$	0.00 [1.02]
11 $[200]\frac{1}{2}^+$	$\frac{1}{2}^+$	0.00 [1.05]

Band mixing is not considered, and the Nilsson orbits in ^{26}Mg are assumed to be filled up to and including orbit 7. The spectroscopic factors given in square brackets are obtained if orbits 9 and 11 are assumed to be filled.

The $\frac{3}{2}^+$ states in ^{25}Na at 90 keV and 2204 keV presumably correspond to the states in ^{23}Na at 0 keV and 2984 keV. The latter states have almost pure calculated components [5]) based on orbits 7 and 9, respectively. The spectroscopic factors $C^2S = 0.11$ and 0.00 from table 4 are not in very good agreement with the observed values of $C^2S = 0.22/0.33$ and 0.15/0.15, respectively. Band mixing and, in particular, about 15 % of excitations in ^{26}Mg into orbit 9 may better account for the observed strength.

A discrepancy seems to exist with respect to the $\frac{1}{2}^+$ states in ^{23}Na (2391 keV, 4431 keV, 6311 keV) and/or ^{25}Na (1068 keV, 3928 keV, 4286 keV). According to Dubois [5]) there exists practically no band mixing for the $\frac{1}{2}^+$ states in ^{23}Na, and they are based on Nilsson orbits 9, 6 and 11, respectively. These assignments are deduced essentially from the very weak population in the ^{22}Ne(τ, d)^{23}Na stripping reaction of the state at 4431 keV which suggests Nilsson orbit 6 for this state. The (d, τ) pick-up reactions leading to ^{23}Na or ^{25}Na populate the energetically lowest $\frac{1}{2}^+$ states at 2391 keV [ref. [1])] or 1068 keV considerably stronger than the other $\frac{1}{2}$ states. This result suggests that the energetically lowest $\frac{1}{2}^+$ states in ^{23}Na and ^{25}Na are the band heads of Nilsson orbit 6 contrary to the assignment of Dubois [5]). Assumed excitations in ^{24}Mg or ^{26}Mg into orbit 9 will not explain the observed behavior. It is not clear yet how this apparent discrepancy can be solved. It is also worth adding that the shell-model estimates for the spectroscopic strengths of the three $\frac{1}{2}^+$ states in ^{25}Na (see table 3) agree very well with an assumed sequence of states based on Nilsson orbits 6, 9 and 11.

The spectroscopic strength, though underestimated in the present experiment, of the transitions in ^{25}Na to the negative-parity states at 3995 keV and 5190 keV suggests that they are the band heads of Nilsson orbits 4 and 2 with $J^\pi = \frac{1}{2}^-$ and $\frac{3}{2}^-$, respectively. Another $\frac{1}{2}^-$ state and two $\frac{3}{2}^-$ states at higher excitation energies are well accounted for.

6. Conclusions and summary

The proton pick-up reaction ^{26}Mg(d, τ)^{25}Na has been used to investigate the nuclear structure of the deformed nucleus ^{25}Na. The measured angular distributions show good agreement with the predictions from the distorted-wave theory. The agreement is improved considerably if couplings to inelastic channels in the initial and final nuclei are included by using the approximate procedure of Kunz *et al.* [11]). Spectroscopic factors have been extracted and were found to be quite sensitive to the details of the calculations, particularly for $l = 0$ transitions. For weaker transitions in reactions on deformed nuclei, spectroscopic factors may be uncertain by a factor of 2. Most spectroscopic factors from the present work agree well with those from other experimental work [1, 9]). Good agreement exists with shell-model predictions [3]) based on a truncated $1d_{\frac{5}{2}}$-$2s_{\frac{1}{2}}$ space. The comparison with predictions from the Nilsson model, though hampered by the apparent lack of band-mixing calculations, shows reasonable agreement except for the spectroscopic strengths leading to the three $\frac{1}{2}^+$ states.

Thanks are due to K. T. Hecht for the careful reading of the manuscript, to P. D. Kunz for making available the computer code DWUCK, and to J. D. Jones for help with the use of his neutron activation equipment.

References

1) E. Krämer, G. Mairle and G. Kaschl, Nucl. Phys. **A165** (1971) 353
2) A. E. Litherland, E. B. Paul, G. A. Bartholomew and H. E. Gove, Phys. Rev. **102** (1956) 208; A. E. Litherland, Third Symp. on the structure of low-medium mass nuclei, 1968, ed. J. P. Davidson (University Press of Kansas) p. 92
3) B. H. Wildenthal, private communication
4) J. A. Becker, R. E. McDonald, L. F. Chase and D. Kohler, Phys. Rev. **188** (1969) 1783
5) J. Dubois, Nucl. Phys. **A104** (1967) 657
6) S. Hinds, H. Marchant and R. Middleton, Nucl. Phys. **31** (1962) 118
7) D. Dehnhard and R. DeLong, Williams Laboratory of Nuclear Physics, University of Minnesota, annual report, 1969;
D. Dehnhard, private communication
8) J. V. Maher, G. C. Morrison, H. T. Fortune and B. Zeidman, Bull. Am. Phys. Soc. **14** (1969) 1201
9) C. Détraz and R. Richter, Nucl. Phys. **A158** (1970) 393
10) H. Rebel *et al.*, Nucl. Phys. **A182** (1972) 145
11) P. D. Kunz, E. Rost and R. R. Johnson, Phys. Rev. **177** (1969) 1737
12) G. T. Kaschl, G. J. Wagner, G. Mairle, U. Schmidt-Rohr and P. Turek, Phys. Lett. **29B** (1969) 167
13) W. C. Parkinson, R. S. Tickle, P. Bruinsma, J. Bardwick and J. M. Lambert, Nucl. Instr. **18** (1962) 93
14) P. D. Kunz, unpublished
15) M. H. MacFarlane and J. B. French, Rev. Mod. Phys. **32** (1960) 567
16) R. H. Bassel, Phys. Rev. **149** (1966) 791
17) E. Newman, L. C. Becker, B. M. Preedom and J. C. Hiebert, Nucl. Phys. **A100** (1967) 225
18) E. F. Gibson, B. W. Ridley, J. J. Kraushaar, M. E. Rickey and R. H. Bassel, Phys. Rev. **155** (1967) 1194

19) B. H. Wildenthal and E. Newman, Phys. Rev. **175** (1968) 1431
20) J. C. Hiebert, E. Newman and R. H. Bassel, Phys. Rev. **154** (1967) 898, and references quoted therein
21) P. M. Endt and C. van der Leun, Nucl. Phys. **105** (1967) 1
22) E. Rost, Phys. Rev. **154** (1967) 994
23) A. S. Broad, Cyclotron Laboratory, University of Michigan, annual report, May 1972, and private communication
24) M. A. Firestone and J. Jänecke, Cyclotron Laboratory, University of Michigan, annual report, May 1972
25) P. Federman, Nucl. Phys. **A95** (1967) 443
26) F. Ajzenberg-Selove, Nucl. Phys. **A190** (1972) 58
27) B. E. Chi, Nucl. Phys. **83** (1966) 97; report, Department of Physics, SUNY at Albany, September 1967